CrossMark

ORIGINAL ARTICLE

AGEs Decreased SIRT3 Expression and SIRT3 Activation Protected AGEs-Induced EPCs' Dysfunction and Strengthened Anti-oxidant Capacity

Mingze Chang,[1,2] Bei Zhang,[1] Ye Tian,[1] Ming Hu,[1] Gejuan Zhang,[2] Zhengli Di,[2] Xinlai Wang,[2] Zhiqin Liu,[1] Naibin Gu,[1] and Yong Liu[1,3]

Abstract—Advanced glycation end products (AGEs) have been confirmed to induce dysfunction in endothelial progenitor cells (EPCs) and play key roles in pathogenesis of diabetes-related vascular complications. The major function of sirtuin 3 (SIRT3) is to orchestrate oxidative metabolism and control reactive oxygen species (ROS) homeostasis, which are more closely related to EPCs' dysfunction. Our study therefore was designed to explore the role of SIRT3 on AGEs-induced EPCs dysfunction of. EPCs isolated from healthy adults were stimulated with AGEs and the expression of SIRT3 was assessed. Then, EPCs transfected with ad-SIRT3 or siRNA-SIRT3 were cultured with or without AGEs. EPCs function, including proliferation, migration; expression of manganese superoxide dismutase (MnSOD), ROS production, and interleukin-8 (IL-8); and vascular endothelial growth factor (VEGF) production were measured. In some experiments, EPCs were pre-cultured with anti-receptor for advanced glycation end products (RAGE) antibody or anti-neutralizing antibody, and then proliferation, migration, expression of MnSOD, ROS production, and IL-8 and VEGF production were measured. Our results showed that SIRT3 expressed in EPCs and AGEs decreased SIRT3 expression. SIRT3 knockdown with siRNA-SIRT3 promoted dysfunction in EPCs whereas SIRT3 activation with ad-SIRT3 strengthened anti-oxidant capacity and protected AGE-impaired dysfunction. Moreover, RAGE may involve in AGEs-decreased SIRT3 expression in EPCs. These data suggested an important role of SIRT3 in regulating EPCs bioactivity.

KEY WORDS: endothelial progenitor cells; SIRT3; AGEs; MnSOD; ROS; RAGE.

INTRODUCTION

Endothelial progenitor cells (EPCs) are circulating cells, mainly characterized by the expression of cell markers CD31, CD133, and vascular endothelial growth factor receptor 2 (VEGFR-2) [1]. In the last decade, a number of studies have demonstrated that EPCs play a pivotal role in the maintenance of endothelial integrity and vascular homeostasis [2]. EPCs are mobilized from the bone marrow into the peripheral blood in response to tissue ischemia or traumatic injury, migrate to sites of injured endothelium, and differentiate into mature endothelial cells in situ [1–3].

Diabetes-associated cardiovascular complications, such as atherosclerosis, myocardial infarction, and stroke, are among the major causes of patient mortality [4]. It has been shown that loss of endothelial integrity contributes to vascular complications of diabetes [5]. However, patients with diabetes and related diseases exhibit a decrease in

---
[1] Institute of Neurobiology, Key Laboratory of Environment and Genes Related to Disease of Education Ministry, Xi'an Jiaotong University School of Medicine, Xi'an, Shaanxi, China
[2] Department of Neurology, Xi'an Central Hospital, Xi'an Jiaotong University School of Medicine, Xi'an, Shaanxi, China
[3] To whom correspondence should be addressed at Institute of Neurobiology, Key Laboratory of Environment and Genes Related to Disease of Education Ministry, Xi'an Jiaotong University School of Medicine, Xi'an, Shaanxi, China. E-mail: xiuyu654@163.com

number and functional capacity of EPCs. Palombo *et al.* [6] have reported that a significant reduction in the number of EPCs is related to carotid intima-media thickness, an induction of early atherosclerosis in diabetes mellitus. Moreover, impaired proliferation, migration, and secretion capacity of EPCs were also reported in patients with diabetes and related diseases [7, 8]. Advanced glycation end products (AGEs), which are produced by the post-translation modification of proteins via non-enzymatic glycation, accumulate with age and abundantly increase in case of diabetes. They have been shown to be deposited in atherosclerotic lesion and to promote diabetes-accelerated atherosclerosis [9, 10]. Cell activation, pro-inflammatory cytokine release, and oxidative stress, induced by the interaction of AGEs with their receptors, may lead to endothelial injury and dysfunction [11, 12]. Previous investigations have demonstrated that AGEs impaired EPCs functions, such as apoptosis, migration, adhesion, and tube formation [13, 14]. However, the underlining mechanism of AGEs impairing EPCs' function still remains largely unknown.

Sirtuin are a conserved family of NAD-dependent ADP-ribosyl transferases and/or protein deacetylases, which are expressed as seven different (SIRT1-SIRT7) isoforms in mammals [15]. They are considered to be key regulator of a wide range of intracellular process, including stress resistance, energy metabolism, apoptosis, and aging [15, 16]. Among these SIRTs, SIRT3 is mainly is targeted to the mitochondrial matrix, where through deacetylation of a variety of substrates—it orchestrates mitochondrial oxidative metabolism and controls reactive oxygen species (ROS) homeostasis [17, 18]. Along these lines, SIRT3 has been reported to prevent detrimental oxidative stress-related phenotypes in a plethora of settings, including cardiac hypertrophy, age-related hearing loss, and ROS-induced embryonic developmental arrest [19–21]. In recent studies, SIRT3 deficiency and the accompanying mitochondrial protein hyperacetylation were reported to be associated with the development of the metabolic syndrome, a cluster of hallmark risk factors for atherosclerosis, including dyslipidemia, glucose intolerance, and central obesity [22]. More importantly, SIRT3 knockdown mice showed diminished angiogenesis and vascular endothelial growth factor (VEGF) and VEGFR-2 expression, which were closely related to EPCs bioactivity [23]. These observations suggested a hypothesis that SIRT3 possibly involve in modulating EPCs bioactivity. This study therefore aims to investigate the role and mechanism of SIRT3 on AGEs-induced EPCs' dysfunction.

MATERIAL AND METHODS

Ethics Statement

This study was approved by the Ethics Committee of Xi'an Central Hospital, Xi'an Jiaotong University School of Medicine, China. Informed consents were obtained from all volunteers and research was conformed to the guidelines of the declaration of Helsinki and its amendments.

EPCs Isolation

EPCs were cultured according to previously described techniques [6]. Briefly, peripheral blood mononuclear cells (PBMCs) from healthy subjects were isolated by Ficoll gradient using Leucosep tubes (Greiner Bio-One, Wemmel, Belgium). After purification with three washing steps, 8×10^6 PBMCs were seeded onto human fibronectin ($2.5 \ mg/cm^2$) pre-coated six-well plates and cultured in endothelial cell basal medium-2 (Clonetics) supplemented with EGM-2 MV single aliquots consisting of 5% FBS, VEGF, fibroblast growth factor-2, epidermal growth factor, insulin-like growth factor-1, and ascorbic acid. The medium was replaced every 3 days, and cells not adhering to the bottom of the culture plates were washed away. On day 7, the cells were changed to serum-free medium for another 24 h and then challenged with AGEs and various interventions, according to experimental protocols.

EPCs Characterization

To verify the EPCs phenotype, the cells were first incubated using Dil-acLDL (10 μg/ml, Molecular probes, USA) for 4 h, fixed with 4% paraformaldehyde, incubated with FITC-labeled lectin (UEA-1, 10 μg/ml, Bios, Beijing, China) for 1 h, and examined using a confocal laser scanning microscope (LSCM, FV-300, Olympus, Japan). Cells that stained positive for both UEA-1 and Dil-acLDL were determined to be EPCs.

EPCs identity was also confirmed by fluorescent-activated cell sorting (FACS) with antibodies recognizing PE-conjugated CD133, FITC-conjugated CD31, and PE-conjugated VEGFR-2, FITC-conjugated CD45 and with the corresponding isotype control antibodies (Bios, Beijing, China). Briefly, cells were harvested using cell dissociation solution and washed twice in phosphate-buffered saline (PBS, Lonza, Verviers, Belgium) supplemented with 1% BSA. Two hundred thousand cells were treated with the appropriate amount of Fc blocking reagent (Miltenyi, Utrecht, The Netherland) and were then stained with specific antibodies or the corresponding isotype control in

50 ml PBS-1% BSA for 30 min at 4 °C. After washing, cells were fixed using the commercial BD FACS lysis solution according to manufacturer's instructions. Twenty thousand to 40,000 events were acquired on a BD FACS-CantoTM flow cytometer and analysis was performed with the FACSDivaTM software (BD Biosciences). Overlays were obtained using FlowJo 7.2.4 software.

Preparations of AGEs with human serum albumin (HSA)

AGEs-HSA was prepared as described previously [13]. Briefly, 2.0 g HSA was dissolved in 10 ml of 0.5 M sodium phosphate buffer (pH 7.4) with 3.0 g of D-glucose. Each sample was sterilized by ultrafiltration, incubated at 37 °C for 8 weeks, and dialyzed against phosphate-buffered saline (pH 7.4). Control non-glycated HSA was incubated in the same conditions except for the absence of reducing sugars. The absence of endotoxin was confirmed by using the Limulus amoebocyte lysate assay (Charles River Laboratories, USA). Protein concentrations were determined with bicinchoninic acid protein assay kit (Boston BioProducts, USA) using bovine serum albumin as a standard. The degree of glycation of the HSA was measured by spectrophotometric assay of pentosidine formation (excitation, 335 nm; emission, 385 nm), and the fluorescence ratio of AGE-HSA to HSA was 2.4. The AGE-HSA was stored under −80 °C and protected from light until used.

RNAi knockdown and adenovirus-mediated overexpression of SIRT3

hSIRT3 (NCBI Reference Sequence: NC 0051093) cDNA expression constructs were chemically synthesized (Neuron Biotech, China). The hSIRT3 cDNA was first subcloned into a pGS-1 vector, and then HEK 293 cells were infected with the ad-SIRT3 recombinant adenovirus in a 12-well plate with MetafecteneTM (Biontex) according to the manufacturer's protocol. Finally, the recombinant ad-SIRT3 was collected 8 days after transfection and amplified in the HEK293T cells, producing 2 ml of viral stock. The adenoviruses expressed GFP under a separate promoter, which allowed the infection to be verified. All PCR-amplified cloning and fragment junctions were confirmed by DNA sequencing (Sangon, Shanghai, China). An adenovirus encoding a green fluorescent protein (ad-control) was used as a control. The ad-SIRT3 and ad-control viruses were used for functional assays. The transfection of ad-SIRT3 was performed according to the manufacturer's instructions. EPCs were transfected with ad-SIRT3 or ad-control constructs for 48 h before being used in experiments.

The siRNA for SIRT3 (human, sc-61555) along with control siRNA (human, sc-44230) and siRNA transfection reagent (human, sc-29528) were purchased from Santa Cruz Biotechnology (Santa Cruz, CA, USA). EPCs were transfected with 100 nM siRNA for 5–7 h according to the manufacturer's protocol. Then, cells were switched into fresh complete medium and incubated for an additional 24 h. Thereafter, cells were harvested for further experiments.

Cell Proliferation Studies

[3H]-thymidine incorporation was used to study EPCs DNA synthesis as previously described [21]. First, EPCs were seeded onto 24-well plates and prepared for different experiments. During the final 6–8 h of treatment, 1 mCi of [methyl-3H]-thymidine was added to each well for 8 h. Finally, incorporated [3H]-thymidine was precipitated with 10% trichloroacetic acid and subsequently counted with a liquid scintillation counter. Furthermore, the cell number (six-well plates, 1×10^6 cells/well as a baseline) was counted after cell treatment. Each count was conducted an average of three times, and every data point was counted in triplicate.

Cell Migration Assay

EPCs migration was evaluated by use of a transwell chamber (6.5 mm diameter inserts, 8.0 mm pore size; Corning, USA). Transwell inserts were placed in a 24-well plate containing EBM-2. EPCs (1×10^5) were added to the upper chamber of the well, without FBS. Cells were allowed to migrate from the upper to the lower chamber for 12 h at 37 μC. Non-migratory cells were removed from the upper chamber by wiping the upper surface with use of an absorbent tip. The number of migrating cells was counted in five different high-power fields per insert.

Measurement of Intracellular Reactive Oxygen Species Levels

The level of intracellular ROS was determined on the basis of the oxidative conversion of cell permeable 2′,7′-dichloro fluorescein diacetate (DCFH-DA, Sigma, USA) to fluorescent dichloro fluorescein (DCF) upon reaction with hydroxyl radical, hydrogen peroxide, or peroxynitrite. Briefly, treatment cells were harvested and washed twice with cold PBS (pH 7.4). Then cells were incubated with 50 mM DCFH-DA at room temperature for 30 min in dark.

Fluorescent signal was recorded by using a fluorescence micros-copy (488 nm filter; Olympus Microscope BX-51, Japan). The fluorescence intensity of eight fields per dish was measured and the ROS level was quantified by measurement of fluorescence intensity with HMIAS-2000 software.

Gene Expression Analysis

Total RNA from cultured cells was isolated using Trizol reagent (Takara Biotechnology, Japan) according to the manufacturer's instructions. cDNA was synthesized using RNA PCR Kit (Takara Biotechnology, Japan) and used as PCR template. Quantitative PCR was performed on ABI PRISM 7900 Sequence Detector system (Applied Biosystems, USA) using SYBR Green I Assay (Takara Biotechnology, Japan). Actin was used as endogenous control. Relative gene expression level (the amount of target, normalized to endogenous control gene) was calculated using the comparative Ct method formula 2-DDCt. The sequences of primers for PCR were listed in Table 1.

Western Blot Analysis

Equal protein amounts were loaded onto SDS-PAGE gels. After running gels, proteins were transferred onto nitrocellulose membranes. Membranes were blocked in 5% nonfat milk and primary antibody incubations were performed with 3% BSA (overnight at 4 °C). Antibodies used were anti-SIRT3 (Santa Cruz, USA), anti-MnSOD (Santa Cruz, USA), and β-actin (Santa Cruz, USA). Then membranes were incubated with peroxidase-conjugated secondary antibodies at room temperature for 2 h. Specific band was detected with chemiluminescence assay (ECL detection reagents, Pierce). Designed software was used to quantify the intensities of bands. Bands were visualized by chemiluminescence detection reagents. Densitometric analysis used Quantity One program (Promega).

MnSOD Activity Assay

MnSOD activity was measured with the MnSOD assay kit using water-soluble tetrazolium salt (WST-1) as a substrate according to the manufacturer's instructions (Abcam).

Assessment of Secretion of IL-8 and VEGF in EPCs

Supernatants were collected and kept frozen at −80 °C until the levels of IL-8 and VEGF were determined by ELISA assays according to the manufacturer's instructions. All commercial kits were purchased from R&D Systems (USA).

Statistical Analysis

Results are shown as mean ± SD of at least three independent experiments. The significance of differences was estimated by ANOVA followed by Student–Newmann–Keuls multiple comparison tests. A value of $p < 0.05$ was considered significant. All statistical analyses were performed with SPSS software (version 17.0).

RESULTS

Characterization of EPCs

Cells began to adhere to the bottom of the well after 24 h culture. Colonies were observed at 48 h and reached a peak on the seventh day. The majority of cultured EPCs ($89.75 \pm 8.40\%$) took up Dil-acLDL and was positively stained with FITC-UEA-1 (Fig. 1). FACS analysis was also used to confirm the endothelial phenotype of the EPCs in the present study. The expression profile of cultured EPCs included VEGFR-2 ($15.8 \pm 6.4\%$), CD31 ($22.4 \pm 10.1\%$), CD133 ($7.1 \pm 4.2\%$), and CD45($84.3\% \pm 10.4\%$).

AGEs Decreased SIRT3 Expression in EPCs

Whether human EPCs express SIRT3 remains unknown. Real-time PCR analysis showed that SIRT3 mRNA was detected in both PBS-treated EPCs and HSA-treated EPCs (Fig. 2a). However, significantly down-regulated SIRT3 mRNA was found in human EPCs incubated with AGEs compared with which in PBS-treated cells (0.32 ± 0.11 *vs.* 1.00 ± 0.00, $p < 0.001$) or HSA-treated cells (0.32

Table 1. Primers

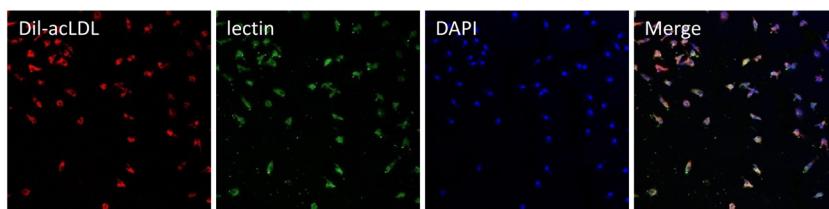| Primer	Forward	Reverse
SIRT3	TCCAATAATGGACAAGTCAAGCC	GCTGTACCCCAGATTTTGTAGCA
MnSOD	GCCTCCCTGACCTGCCTTAC	GTGATTGATATGGCCCCCG
β-actin	GTGATTGATATGGCCCCCG	CCAGAGGCATACAGGGACAAC

Fig. 1. Characterization of EPCs. Representative pictures of dual-stained EPCs with Dil-acLDL (*red*) and UEA-1 (*green*) (magnification ×100).

± 0.11 *vs.* 0.89 ± 0.15, $p < 0.001$). Furthermore, there was no statistically difference in SIRT3 mRNA between PBS-treated EPCs and HSA-treated cells (1.00 ± 0.00 *vs.* 0.89 ± 0.15, $p > 0.5$) (Fig. 2a). Western blot analysis showed a similar result that SIRT3 protein highly expressed in EPCs, but was statistically down-regulated in AGEs-treated EPCs compared in PBS-treated cells ($p < 0.001$) or HSA-treated cells ($p < 0.001$) (Fig. 2b).

To obtain further more details between SIRT3 and AGEs, EPCs was stimulated with 50, 200, or 500 μg/ml AGEs and cells were harvested at different incubation time. Our results found that AGEs decreased SIRT3 mRNA and protein in a dose and time manner (Fig. 3). As illustrated in Fig. 3a, c, SIRT3 mRNA was only 0.32-fold after EPCs stimulated with 500 μg/ml AGEs for 24 h. The similar results were obtained in SIRT3 protein with Western blot analysis.

SIRT3 Activation Protected AGEs-Impaired EPCs Proliferation and Migration

Next, we explore the effects of SIRT3 on AGEs-treated EPCs' dysfunction. First, EPCs were trans-

fected with ad-SIRT3 to supplement down-regulation of SIRT3 in AGEs-treated EPCs. Adenovirus constructs expressing ad-control or ad-SIRT3 were transfected into the EPCs. After 48 h, the transfection efficiency of the adenovirus constructs as calculated by GFP expression was 82.3 ± 3.5 and 85.1 ± 4.4% (ad-control and ad-SIRT3), respectively. The SIRT3 expression levels were determined by western blotting and quantitative RT-PCR 48 h after transfection. RT-PCR showed that transfected with ad-control did not alter SIRT3 expression whereas transfected with ad-SIRT3 largely increased SIRT3 mRNA from 0.92 ± 0.11 to 1.80 ± 0.25 ($p < 0.001$). Furthermore, western blotting showed that compared with ad-control group, transfected with ad-SIRT3 significantly increased SIRT3 protein in EPCs ($p < 0.001$) (Fig. 4a). These results showed that transfected with ad-SIRT3 were effective in human EPCs.

Then, we explore the effects of SIRT3 on AGEs-induced EPCs' dysfunction. After transfected with/without ad-SIRT3 or ad-control for 48 h, EPCs were stimulated with PBS or AGEs for 24 h. Again, SIRT3
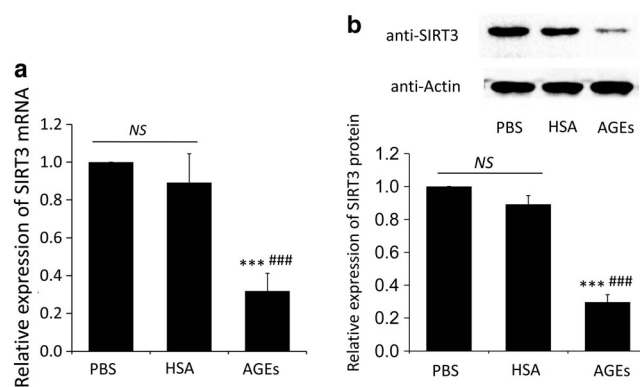

Fig. 2. AGEs decreased the expression of SIRT3 in EPCs. EPCs were cultured with PBS, HSA (500 μg/ml), or AGEs (500 μg/ml) for 24 h. **a** SIRT3 mRNA levels were measured by qualitative RT-PCR analysis ($n = 6$). **b** SIRT3 protein levels were measured by western blot analysis. *Top*, SIRT3 protein expression levels normalized to the expression levels of the housekeeping gene β-actin. *Bottom*, densitometric analysis of the SIRT3 protein expression levels relative to β-actin was determined by the Quantity One program ($n = 3$). Data are presented as mean ± SD. (* indicated *vs.* cells cultured with PBS, ***$p < 0.001$. # indicated *vs.* cells cultured with HSA. ###$p < 0.001$. *NS*, non-significant).
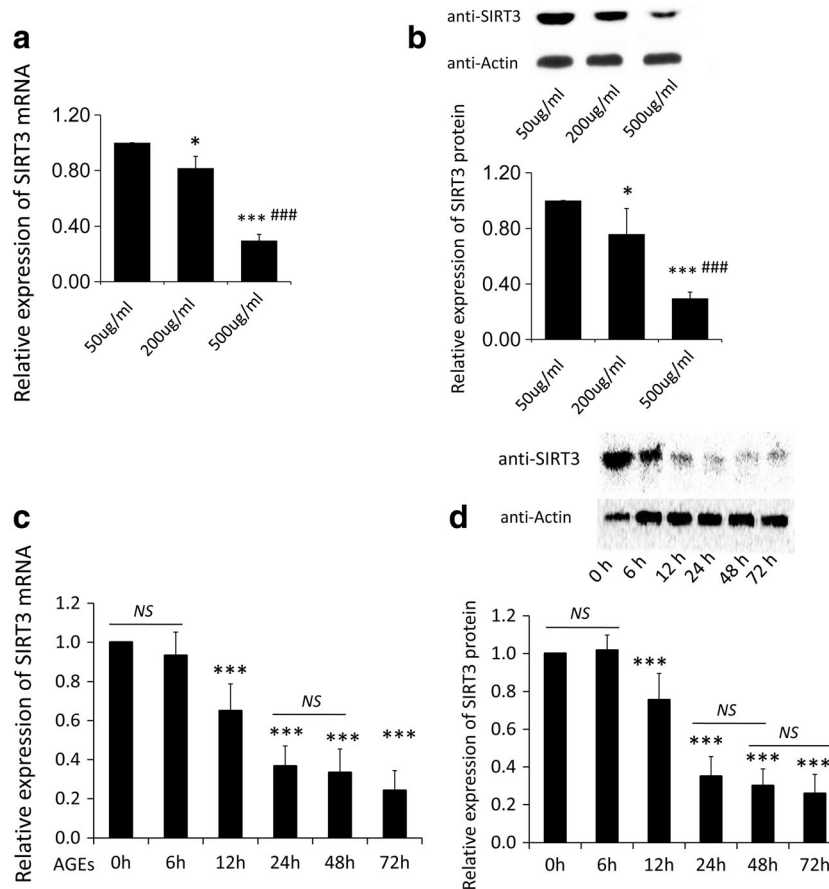
Fig. 3. AGEs decreased SIRT3 expression in EPCs in a dose- and time-dependent manner. In dose-dependent experiment, EPCs were cultured with AGEs (50, 200, or 500 μg/ml) for 24 h. In time-dependent experiment, EPCs were cultured with 500 μg/ml AGEs for indicated incubation time. **a, c** SIRT3 mRNA levels were measured by qualitative RT-PCR analysis ($n = 6$). **b, d** SIRT3 protein levels were measured by western blot analysis. *Top*, SIRT3 protein expression levels normalized to the expression levels of the housekeeping gene β-actin. *Bottom*, densitometric analysis of the SIRT3 protein expression levels relative to β-actin was determined by the Quantity One program ($n = 3$). Data are presented as mean ± SD of at least three independent experiments. (* indicated *vs.* cells cultured with PBS, *$p < 0.05$, ***$p < 0.001$. # indicated *vs.* cells cultured with HSA. ###$p < 0.001$. *NS*, non-significant).

mRNA was measured in these different cultures. Our results found that AGEs significantly decreased SIRT3 mRNA ($p < 0.001$). However, compared with ad-control, transfected with ad-SIRT3 significantly reversed AGEs-decreased SIRT3 mRNA in EPCs ($p < 0.001$) (Fig. 4b).

[3H]-thymidine analysis was then used to measure the proliferation of EPCs. Consistent with previous studies, our results showed that AGEs significant decreased EPCs proliferation, as shown by the decreased uptake of [3H]-thymidine significantly from 3033.33 ± 377.71 in PBS-treated EPCs to 1200.58 ± 180.12 in AGEs-treated cells ($p < 0.001$) (Fig. 4c). However, transfected with ad-SIRT3 largely reversed AGEs impaired uptake of [3H]-thymidine from 1426.56 ± 212.14 to 2552.65 ± 172.28 ($p < 0.001$) (Fig. 4c).

Migration assay showed that compared with PBS-treated cells, AGEs also significantly impaired EPCs migration ($p < 0.001$) (Fig. 4d). More importantly, transfected with ad-SIRT3 largely blocked AGEs-impaired EPCs migration, as shown by the increased cell numbers from (1.47 ± 0.12) × 10^5 to (2.34 ± 0.21) × 10^5 ($p < 0.001$) (Fig. 4d).

Effects of AGEs on the Productions of IL-8 and VEGF in EPCs

The release of angiogenic factors by EPCs also contributes to the vasculature integrity and homeostasis. Next, the amounts of IL-8 and VEGF released from the EPCs were measured in our study. The results showed that
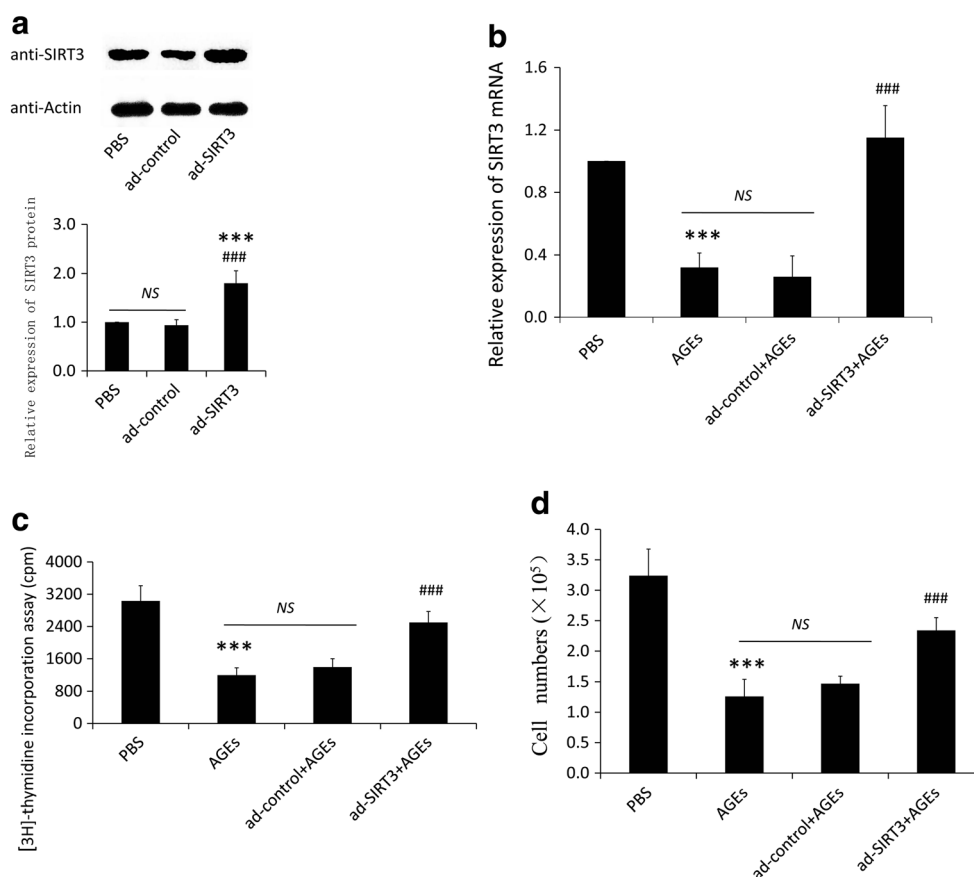
Fig. 4. SIRT3 protected AGEs-impaired proliferation and migration in EPCs. EPCs were transfected with ad-SIRT3 or ad-control for 48 h. **a** SIRT3 mRNA levels were measured by qualitative RT-PCR analysis ($n = 6$). Data are presented as mean ± SD. (* indicated *vs.* cells cultured with PBS, ***$p < 0.001$. # indicated *vs.* cells transfected with ad-control, ###$p < 0.001$. *NS*, non-significant). EPCs were treated with PBS or AGEs (500 μg/ml) for 24 h after transfected. **b** SIRT3 mRNA levels were measured by qualitative RT-PCR analysis ($n = 6$). **c** EPCs proliferation was measured by the uptake of [3H]-thymidine ($n = 5$). **d** EPCs transfected with ad-SIRT3 or ad-control were treated by 500 μg/ml for 24 h before transfer to the top of a transwell chamber. The number of migrating cells was counted in five different high-power fields per insert after 12 h ($n = 5$). Data are presented as mean ± SD. (* indicated *vs.* cells cultured with PBS, ***$p < 0.001$. # indicated *vs.* cells transfected with ad-control, ###$p < 0.001$. *NS*, *non*-significant).

compared with PBS-treated cells, AGEs significantly impaired the release of IL-8 and VEGF (all $p < 0.001$) (Fig. 5a, b). More importantly, transfected with ad-SIRT3 largely increased the amounts of IL-8 and VEGF in AGEs-treated EPCs (all $p < 0.001$) (Fig. 5a, b).

SIRT3 Knockdown Lead to EPCs Dysfunction

To explore whether SIRT3 has a direct effect on EPCs function, EPCs were transfected with siRNA-SIRT3 or siRNA-control and EPCs function, including proliferation, migration, and secretion capacity of EPCs were measured. The transfection efficiency of siRNA-SIRT3 was measured by quantitative RT-PCR. RT-PCR found that transfection with siRNA-control did not alter SIRT3 expression in EPCs ($p > 0.05$) whereas transfection with siRNA-SIRT3 largely decreased SIRT3 mRNA from 0.93 ± 0.15 to 0.32 ± 0.05 ($p < 0.001$). [3H]-thymidine analysis showed that compared with siRNA-control, EPCs transfected with siRNA-SIRT3 largely impaired uptake of [3H]-thymidine from 2754.22 ± 251.68 to 1511.86 ± 202.33 ($p < 0.001$) (Fig. 6a).

Migration assay showed a similar result. Transfection with siRNA-SIRT3 significantly decreased cell numbers ($p < 0.001$) (Fig. 6b), whereas transfection with siRNA-control did not alter cells numbers in the lower chamber ($p > 0.05$) (Fig. 6b). Angiogenic secretion analysis showed that compared with siRNA-control, EPCs transfected with siRNA-SIRT3 largely impaired the amounts of IL-8 and VEGF in EPCs (all $p < 0.001$) (Fig. 6c, d).
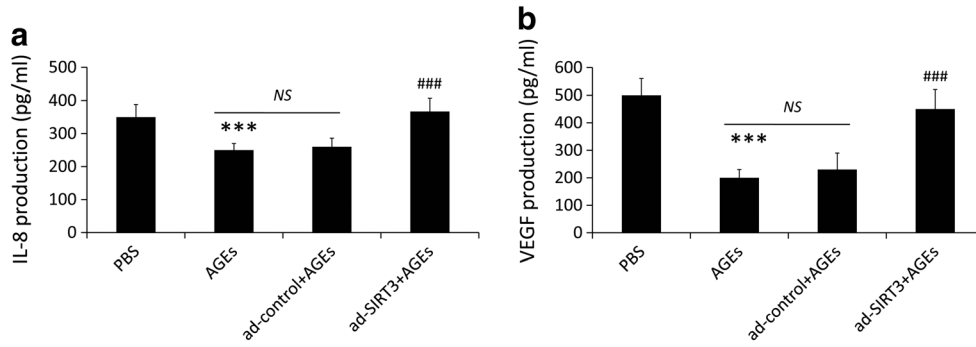
Fig. 5. SIRT3 reversed AGEs-impaired IL-8 and VEGF production in EPCs. EPCs were treated with PBS or AGEs (500 μg/ml) for 24 h after transfection. Supernatant in the cultures were collected and tested for IL-8 and VEGF by ELISA ($n = 6$). Data are presented as mean ± SD. (* indicated *vs.* cells cultured with PBS, **p <0.01. # indicated *vs.* cells transfected with ad-control, ###p < 0.001. *NS*, non-significant).

SIRT3 Protected AGEs-Induced EPCs Dysfunction by Strengthening Anti-oxidant Capacity

To unveil the mechanism of SIRT3 regulating AGEs-EPCs' function, ROS levels and MnSOD expression and activity were measured in our study. Our results found that compared with PBS-treated EPCs, AGEs promoted significant ROS production in EPCs ($p < 0.001$) (Fig. 7a). However, transfected with ad-SIRT3 markedly decreased ROS production compared with ad-control group ($p < 0.001$) (Fig. 7a). Figure 7b showed that MnSOD protein was decreased in AGEs-treated cells while transfected with SIRT3 markedly reversed the expression of
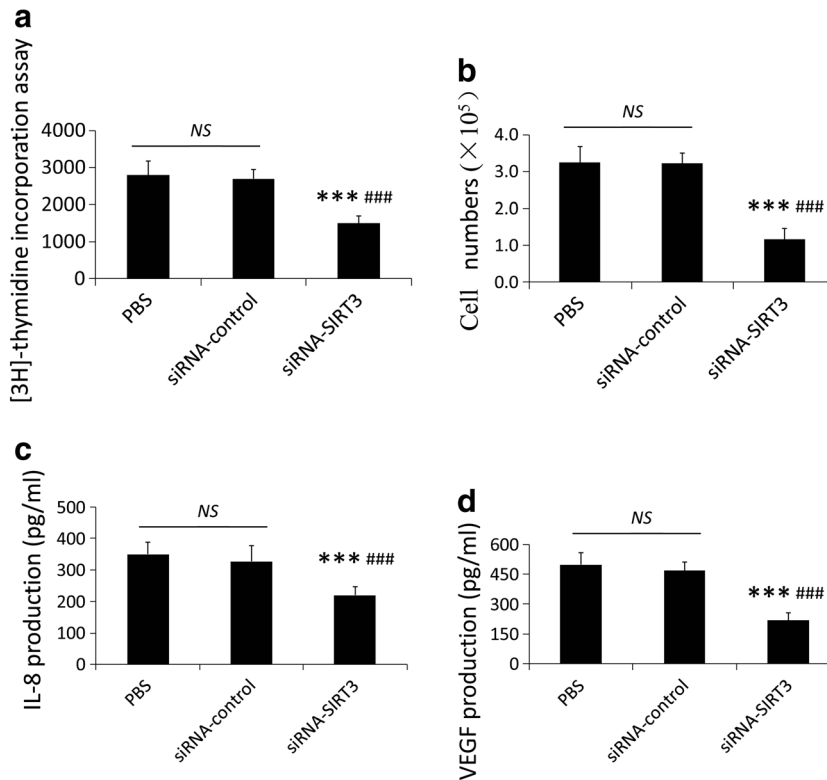

Fig. 6. SIRT3 knockdown lead to EPCs dysfunction. EPCs were transfected with siRNA-SIRT3 or siRNA-control for 24 h. **a, b** The proliferation and migration of EPCs were measured with respective methods ($n = 6$). **c, d** Cytokines levels of IL-8 and VEGF were measured by ELISA ($n = 6$). Data are presented as mean ± SD. (* indicated *vs.* cells cultured with PBS, ***$p < 0.001$. # indicated *vs.* cells transfected with siRNA-control, #$p < 0.05$, ###$p < 0.001$. *NS*, non-significant).
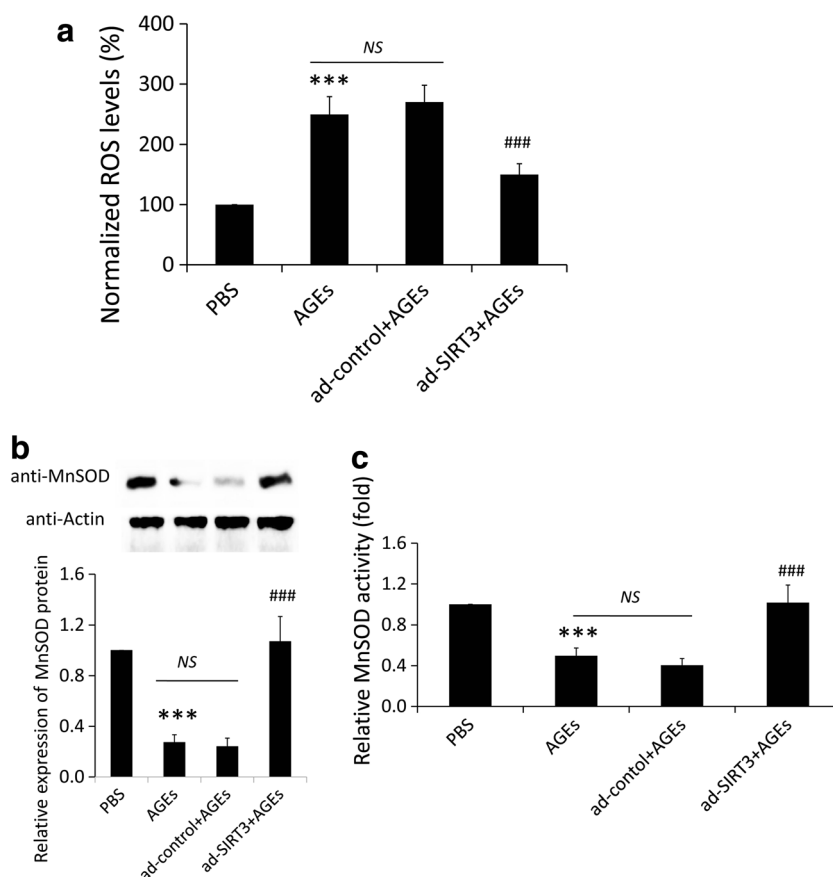
Fig. 7. SIRT3 strengthened anti-oxidized capacity in AGEs-treated EPCs. EPCs were cultured as described in legend 5. **a** The intracellular ROS production was measured by DCFH-DA fluorescence dye ($n = 6$). **b** MnSOD protein levels were measured by western blot analysis. *Top*, MnSOD protein expression levels normalized to the expression levels of the housekeeping gene β-actin. *Bottom*, Densitometric analysis of the MnSOD protein expression levels relative to β-actin was determined by the Quantity One program ($n = 3$). **c** MnSOD activity was measured with SOD assay kit ($n = 4$). Data are presented as mean ± SD. * indicated *vs*. cells cultured with PBS, ***$p < 0.001$. # indicated *vs*. cells transfected with ad-control, ###$p < 0.001$. *NS*, non-significant.

MnSOD protein in AGEs-treated EPCs ($p < 0.001$). Moreover, MnSOD enzyme activity was decreased in AGEs-treated cells while transfected with ad-SIRT3 increased 2.67-fold MnSOD enzyme activity in AGEs-treated cells compared with ad-control ($p < 0.001$) (Fig. 7c).

The Involvement of RAGE in Regulating SIRT3 in EPCs

To investigate whether RAGE were involved in the down-regulation of SIRT3 in EPCs by AGEs, EPCs were pretreated with anti-RAGE antibody or anti-neutralizing antibody, then cells were stimulated with 500 μg/ml AGEs for 24 h and the expression of SIRT3 was measured. Our study found that compared with non-specific neutralizing antibody, pretreatment with specific anti-RAGE antibody significantly reversed AGEs-decreased expression of SIRT3 mRNA and protein (all $p < 0.01$) (Fig. 8a, b). However, non-specific neutralizing antibody had no effects on the down-regulation of SIRT3 mRNA and protein by AGEs (Fig. 8a, b).

The effects of anti-RAGE antibody on AGEs-induced dysfunction also were measured. Figures 8b and 9a showed compared with non-specific neutralizing antibody, pretreatment with specific anti-RAGE antibody significantly reversed AGEs-impaired EPCs proliferation and migration (all $p < 0.001$). A similar effect of anti-RAGE antibody on AGEs-impaired IL-8 and VEGF production in EPCs was also obtain in our study (Fig. 9c, d). Pretreatment with specific anti-RAGE antibody could largely reversed AGEs-impaired IL-8 and VEGF production in EPCs ($p < 0.01$ and $p < 0.001$, respectively). Furthermore, ROS
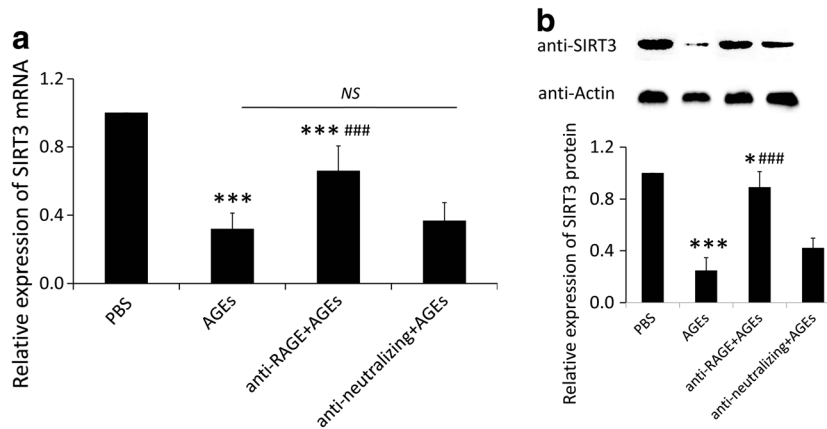
Fig. 8. The involvement of RAGE in AGEs-decreased SIRT3 expression in EPCs. EPCs were pre-cultured with anti-RAGE antibody (20 μg/ml) or non-specific anti-neutralizing antibody (20 μg/ml) for 2 h, and then cells were stimulated with AGEs (500 μg/ml) for 24 h. **a** SIRT3 mRNA levels were measured by qualitative RT-PCR analysis ($n = 6$). **b** SIRT3 protein levels were measured by western blot analysis. *Top*, SIRT3 protein expression levels normalized to the expression levels of the housekeeping gene β-actin. *Bottom*, Densitometric analysis of the SIRT3 protein expression levels relative to β-actin was determined by the Quantity One program ($n = 3$). Data are presented as mean ± SD. (* indicated *vs.* cells cultured with PBS, *$p < 0.05$, ***$p < 0.001$. # indicated *vs.* cells pre-cultured with non-specific anti-neutralizing antibody, ###$p < 0.001$. *NS*, non-significant).

production and MnSOD enzyme activity were also detected in EPCs pre-cultured with anti-RAGE antibody. Our results showed that compared with non-specific neutralizing antibody, pre-cultured with specific anti-RAGE antibody could largely decreased ROS production and increased MnSOD enzyme activity (all $p < 0.001$) (Fig. 9e, f).

DISCUSSION

The present study was to investigate the role of SIRT3 in AGEs-induced EPCs' dysfunction. Specially, our investigation revealed that (1) SIRT3 expressed in EPCs and AGEs decreased SIRT3 expression and induced EPCs dysfunction; (2) SIRT3 activation reversed AGEs-induced EPCs dysfunction, including proliferation, migration and angiogenic secretion. (3) Moreover, SIRT3 activation in AGEs-treated EPCs' strengthened its anti-oxidant capacity, decreased ROS production, and increased MnSOD expression and activity. (4) RAGE were involved in AGEs-induced decrease in SIRT3 expression, ROS production, and EPCs dysfunction.

As an important source of renewing injured endothelial cells, decreased peripheral EPCs numbers and impaired EPCs function have been shown to correlate with endothelial dysfunction and diabetes [7]. Recent observations suggest that EPCs could be sub-populated as early and late outgrowth EPCs [24, 25]. The early EPCs appear within 4 to 7 days while the late EPCs develop after 2 to 3 weeks in

ex vivo culture systems. They share some endothelial phenotype but are identified with different morphology, proliferation rate, and survival feature. In this study, we identified early EPCs with expressing CD31, CD133, VEGFR-2, and CD45. These results were consistent with early EPCs identification in previous studies [24, 25].

Previous investigations have demonstrated that AGEs impair EPCs functions, such as apoptosis, migration, adhesion, and tube formation [13, 14]. In agreement with these findings, we have here shown that a dose of 500 μg/ml AGEs significantly impaired EPCs function, including proliferation, migration, and angiogenic cytokines secretion. These results raised a question what the mechanisms behind this might be.

SIRT3, a mitochondrial sirtuin, appears to be the primary mediator of mitochondrial acetylation, since no significant changes in acetylation status are detectable in mice lacking SIRT4 and SIRT5 [17]. Previous studies have reported that SIRT3 respond to ox-LDL or high glucose expressed in human endothelial cells [26, 27]. Little is known about expression of SIRT3 in EPCs. In the present study, we first demonstrated that SIRT3 expressed in EPCs. More importantly, AGEs stimulation induced dose- and time-dependent decrease in SIRT3 expression.

SIRT3 activation attenuated oxidized low-density lipoprotein-induced human umbilical vein endothelial cells' apoptosis [26]. SIRT3 activation also reduces lipid accumulation in human hepatic cells via AMPK activation [28]. However, our results found that SIRT3 knockdown
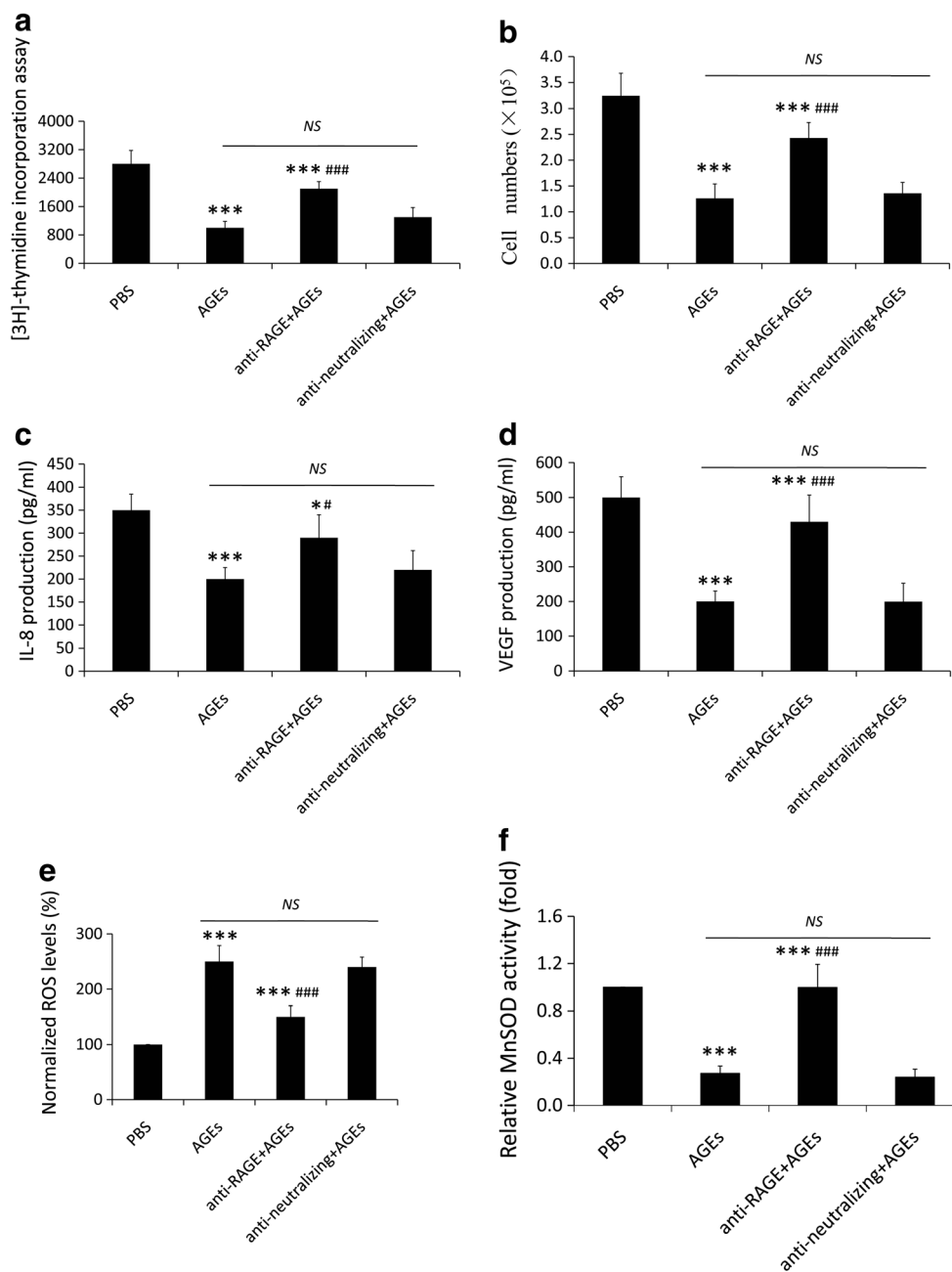
Fig. 9. The involvement of RAGE in AGEs-induced EPCs dysfunction, ROS production, and MnSOD activity. EPCs were cultured as described in legend 7. **a**, **b** The proliferation and migration of EPCs were measured with respective methods ($n = 6$). **c**, **d** Cytokines levels of IL-8 and VEGF were measured by ELISA ($n = 6$). **e** The intracellular ROS production was measured by DCFH-DA fluorescence dye ($n = 6$). **f** MnSOD activity was measured with SOD assay kit ($n = 4$). Data are presented as mean ± SD. (* indicated *vs*. cells cultured with PBS, *$p < 0.05$, ***$p < 0.001$. # indicated *vs*. cells pre-cultured with non-specific anti-neutralizing antibody, #$p < 0.05$, ###$p < 0.001$. *NS*, non-significant).

largely impaired EPCs' function, including proliferation and migration. To know whether the decrease in SIRT3 contributed for AGEs-induced EPCs' dysfunction, we over-expressed SIRT3 with ad-SIRT3. Our results found that SIRT3 activation largely reversed AGEs-impaired proliferation and migration in EPCs. Results collectively

indicate that SIRT3 is an important factor in controlling EPCs biological behavior.

A role of SIRT3 in regulation of cellular ROS levels has been documented before. SIRT3 governs the detoxification of cellular ROS by regulating anti-oxidant enzymes. *In vitro* and *in vivo* SIRT3-mediated deacetylation and activation of MnSOD reduced cellular ROS levels [29, 30]. It is demonstrated that SIRT3-mediated activation of Foxo3a augmented the transcription of both MnSOD and catalase (Cat), thereby preventing mitochondrial ROS accumulation in cardiomyocytes [21]. In the present study, our data showed that AGEs decreased MnSOD expression and activity and promoted ROS production whereas SIRT3 activation with ad-SIRT3 increased MnSOD expression and activity, and decreased ROS production. ROS are widely employed second messengers involved in cell death, pro-inflammatory responses, growth stimulatory events, and other signaling processes that alter the physiological state of the cell. Studies have confirmed that ROS induced EPCs dysfunction via AMPK/p38/NF-kappaB signaling pathway [28, 31]. Although gene loss technology was not use in our study to explore the effect of SIRT3 on ROS production and EPCs' dysfunction, several studies have reported that loss of SIRT3 triggers ROS and oxidative damage, affecting distinct cellular processes and promoting phenotypes of aging [30, 32]. Therefore, it is speculated that AGEs decreased SIRT3 expression in EPCs, which subsequently triggered ROS and oxidative damage, leading to EPCs' dysfunction.

EPCs keep endothelial integrity not only by differentiating into mature vascular endothelial cells but also by secreting the soluble factors including a number of enzymes like matrix protein, growth factors, and cytokines. Compared with late EPCs, early EPCs-like cells secreted angiogenic cytokines such as VEGF, HGF, G-CSF, and IL-8, which might activate adjacent endothelial cells and enhance angiogenesis [25]. VEGF has a stimulatory effect on EPCs proliferation and is a potent stimulator of vasculogenesis, unique retinal pathways for VEGF regulation may be sufficient to overcome EPCs dysfunction resulting in diabetic retino pathy [33]. IL-8 is a relevant chemokine for EPCs homing [34]. We also checked IL-8 and VEGF in EPCs. Our results showed that AGEs significantly decreased IL-18 and VEGF in EPCs whereas SIRT3 activation rescued AGEs-impaired secretion of IL-8 and VEGF. Furthermore, SIRT3 knock-down directly impaired the secretion capacity of IL-8 and VEGF. These results suggested that an important role of SIRT3 on EPCs not only limit on the proliferation and migration but also affect the secretion of angiogenic factors.

Another central question of the study was the mechanism involved in AGEs-decreased expression of SIRT3.

AGEs linked to cellular stress and tissue dysfunction include receptor-independent and receptor-dependent processes. The interaction of AGE with its receptor RAGE results in various reactions, including activation of nuclear factor-kB or mitogen-activated protein kinases (MAP-kinases), increased expression of inflammatory cytokines and adhesion molecules, and induction of oxidative stress [35, 36]. Expression of RAGEs on EPCs surface had been described previously [15, 36]. Here, we found that specific anti-SIRT3 neutralizing antibody largely reversed AGEs inhibited SIRT3 expression and reversed AGEs-impaired EPCs dysfunction, suggesting that receptor-dependent manner contributed largely to the decreased SIRT3 expression in EPCs.

In conclusion, this study provided evidence to demonstrate that AGEs decrease SIRT3 and promoted dysfunction in EPCs, whereas SIRT3 activation strengthen anti-oxidant capacity and protected AGEs-impaired dysfunction. Furthermore, RAGE may involve in AGEs-induced decrease SIRT3 expression and dysfunction in EPCs. These data collectively suggested an important role of SIRT3 in regulating EPCs bioactivity.

COMPLIANCE WITH ETHICAL STANDARDS

Conflict of Interest. All authors declare that they have no conflict of interest.

REFERENCES

1. Urbich, C., and S. Dimmeler. 2004. Endothelial progenitor cells: characterization and role in vascular biology. *Circulation Research* 95: 343–353.
2. Rabelink, T.J., H.C. de Boer, E.J. de Koning, and A.J. van Zonneveld. 2004. Endothelial progenitor cells: more than an inflammatory response. *Arteriosclerosis, Thrombosis, and Vascular Biology (Dallas, TX)* 24: 834–838.
3. Groleau, J., S. Dussault, P. Haddad, J. Turgeon, C. Menard, J.S. Chan, and A. Rivard. 2010. Essential role of copper- zinc superoxide dismutase for ischemia-induced neovascularization via modulation of bone marrow-derived endothelial progenitor cells. *Arteriosclerosis, Thrombosis, and Vascular Biology (Dallas, TX)* 30: 2173–2181.
4. Heller, G.V. 2005. Evaluation of the patient with diabetes mellitus and suspected coronary artery disease. *The American Journal of Medicine* 118: 9S–14S.
5. Waltenberger, J. 2001. Impaired collateral vessel development in diabetes: potential cellular mechanisms and therapeutic implications. *Cardiovascular Research* 49: 554–560.
6. Palombo, C., M. Kozakova, C. Morizzo, L. Gnesi, M.C. Barsotti, P. Spontoni, F. Massart, P. Salvi, A. Balbarini, G. Saggese, et al. 2011.

Circulating endothelial progenitor cells and large artery structure and function in young subjects with uncomplicated type 1 diabetes. *Cardiovascular Diabetology* 10: 88.

7. Tepper, O.M., R.D. Galiano, J.M. Capla, et al. 2002. Human endothelial progenitor cells from type II diabetics exhibit impaired proliferation, adhesion, and incorporation into vascular structures. Circulation 106:2781–6

8. Vasa, M., S. Fichtlscherer, A. Aicher, et al. 2001. Number and migratory activity of circulating endothelial progenitor cells inversely correlate with risk factors for coronary artery disease. *Circulation Research* 89: E1–E7.

9. Jandeleit-Dahm, K., A. Watson, and A. Soro-Paavonen. 2008. The AGEs/RAGEs axis in diabetes-accelerated atherosclerosis. *Clinical and Experimental Pharmacology and Physiology* 35: 329–334.

10. Moriyama, T., M. Kemi, C. Okumura, K. Yoshihara, and T. Horie. 2010. Involvement of advanced glycation end-products, pentosidine and N(epsilon)-(carboxymethyl)lysine, in doxorubicin-induced cardiomyopathy in rats. *Toxicology* 268: 89–97.

11. Madonna, R., and R. de Caterina. 2011. Cellular and molecular mechanisms of vascular injury in diabetes—part II: cellular mechanisms and therapeutic targets. *Vascular Pharmacology* 54: 75–79.

12. Zhou, Y.J., H.W. Yang, X.G. Wang, and H. Zhang. 2009. Hepatocyte growth factor prevents advanced glycation end products-induced injury and oxidative stress through a PI3K/Akt-dependent pathway in human endothelial cells. *Life Sciences* 85: 670–677.

13. Chen, J., M. Song, S. Yu, P. Gao, Y. Yu, H. Wang, and L. Huang. 2010. Advanced glycation endproducts alter functions and promote apoptosis in endothelial progenitor cells through receptor for advanced glycation endproducts mediate overpression of cell oxidant stress. *Molecular and Cellular Biochemistry* 335: 137–146.

14. Li, H., X. Zhang, X. Guan, X. Cui, Y. Wang, H. Chu, and M. Cheng. 2012. Advanced glycation end products impair the migration, adhesion and secretion potentials of late endothelial progenitor cells. *Cardiovascular Diabetology* 11: 46.

15. Finkel, T., C.X. Deng, and R. Mostoslavsky. 2009. Recent progress in the biology and physiology of sirtuin. *Nature* 460: 587–591.

16. Schwer, B., and E. Verdin. 2008. Conserved metabolic regulatory functions of sirtuins. *Cell Metabolism* 7: 104–112.

17. Lombard, D.B., F.W. Alt, H.L. Cheng, J. Bunkenborg, R.S. Streeper, R. Mostoslavsky, J. Kim, G. Yancopoulos, D. Valenzuela, A. Murphy, Y. Yang, Y. Chen, M.D. Hirschey, R.T. Bronson, M. Haigis, L.P. Guarente, R.V. Farese, S. Weissman, E. Verdin, and B. Schwer. 2007. Mammalian Sir2 homolog SIRT3 regulates global mitochondrial lysine acetylation. *Molecular and Cellular Biology* 27: 8807–8814.

18. Tseng, A.H., S.S. Shieh, and D.L. Wang. 2013. SIRT3 deacetylates FOXO3 to protect mitochondria against oxidative damage. *Free Radical Biology and Medicine* 63: 222–234.

19. Sundaresan, N.R., M. Gupta, G. Kim, S.B. Rajamohan, A. Isbatan, and M.P. Gupta. 2009. Sirt3 blocks the cardiac hypertrophic response by augmenting Foxo3a-dependent antioxidant defense mechanisms in mice. *Journal of Clinical Investigation* 119: 2758–2771.

20. Hirschey, M.D., T. Shimazu, E. Jing, C.A. Grueter, A.M. Collins, B. Aouizerat, A. Stancakova, E. Goetzman, M.M. Lam, B. Schwer, R.D. Stevens, M.J. Muehlbauer, S. Kakar, N.M. Bass, J. Kuusisto, M. Laakso, F.W. Alt, C.B. Newgard, R.V. Farese Jr., C.R. Kahn, and E. Verdin. 2011. Sirt3 deficiency and mitochondrial protein hyperacetylation accelerate the development of the metabolic syndrome. *Molecular Cell* 44: 177–90.

21. Zeng, H., X. He, X. Hou, L. Li, and J.X. Chen. 2014. Apelin gene therapy increases myocardial vascular density and ameliorates diabetic cardiomyopathy via upregulation of sirtuin 3. *American Journal of Physiology. Heart and Circulatory Physiology* 306: 585–597.

22. Cheng, C.C., S.J. Chang, Y.N. Chueh, T.S. Huang, P.H. Huang, S.M. Cheng, T.N. Tsai, J. Chen, and H.W. Wang. 2013. Distinct angiogenesis roles and surface markers of early and late endothelial progenitor cells revealed by functional group analyses. *BMC Genomics* 14: 182.

23. Hur, J., C.H. Yoon, H.S. Kim, J.H. Choi, H.J. Kang, K.K. Hwang, B.H. Oh, M.M. Lee, and Y.B. Park. 2004. Characterization of two types of endothelial progenitor cells and their different contributions to neovasculogenesis. *Arteriosclerosis, Thrombosis, and Vascular Biology (Dallas, TX)* 24: 288–293.

24. Luo, X., Z. Yang, S. Zheng, Y. Cao, and Y. Wu. 2014. Sirt3 activation attenuated oxidized low-density lipoprotein-induced human umbilical vein endothelial cells' apoptosis. *Cell Biology International* 24: 288–293.

25. Mortuza, R., S. Chen, B. Feng, S. Sen, and S. Chakrabarti. 2013. High glucose induced alteration of SIRTs in endothelial cells causes rapid aging in a p300 and FOXO regulated pathway. *PloS One* 8, e54514.

26. Shi, T., G.Q. Fan, and S.D. Xiao. 2010. SIRT3 reduces lipid accumulation in human hepatic cells via AMPK activation. *Journal of Digestive Diseases* 11: 55–62.

27. Chen, Y., J. Zhang, Y. Lin, Q. Lei, K.L. Guan, S. Zhao, and Y. Xiong. 2011. Tumour suppressor SIRT3 deacetylates and activates manganese superoxide dismutase to scavenge ROS. *EMBO Reports* 12: 534–541.

28. Qiu, X., K. Brown, M.D. Hirschey, E. Verdin, and D. Chen. 2010. Calorie restriction reduces oxidative stress by SIRT3-mediated SOD2 activation. *Cell Metabolism* 12: 662–667.

29. Ji, K.T., L. Qian, J.L. Nan, Y.J. Xue, S.Q. Zhang, G.Q. Wang, R.P. Yin, Y.J. Zhu, L.P. Wang, J. Ma, L.M. Liao, and J.F. Tang. 2015. Ox-LDL induces dysfunction of endothelial progenitor cells via activation of NF-kappaB. *BioMed Research International* 2015: 175291.

30. Someya, S., W. Yu, W.C. Hallows, J. Xu, J.M. Vann, C. Leeuwenburgh, M. Tanokura, J.M. Denu, and T.A. Prolla. 2010. Sirt3 mediates reduction of oxidative damage and prevention of age-related hearing loss under caloric restriction. *Cell* 143: 802–812.

31. Iwaguro, H., J. Yamaguchi, C. Kalka, et al. 2002. Endothelial progenitor cell vascular endothelial growth factor gene transfer for vascular regeneration. *Circulation* 105: 732–738.

32. Kocher, A.A., M.D. Schuster, M. Bonaros, K. Lietz, G. Xiang, T.P. Martens, P.A. Kurlansky, H. Sondermeijer, P. Witkowski, A. Boyle, S. Homma, S.F. Wang, and S. Itescu. 2006. Myocardial homing and neovascularization by human bone marrow angioblasts is regulated by IL-8/Gro CXC chemokines. *Journal of Molecular and Cellular Cardiology* 40: 455–464.

33. Sun, C., C. Liang, Y. Ren, Y. Zhen, Z. He, H. Wang, H. Tan, X. Pan, and Z. Wu. 2009. Advanced glycation end products depress function of endothelial progenitor cells via p38 and ERK 1/2 mitogen-activated protein kinase pathways. *Basic Research in Cardiology* 104: 42–49.

34. Scheubel, R.J., S. Kahrstedt, H. Weber, J. Holtz, I. Friedrich, J. Borgermann, R.E. Silber, and A. Simm. 2006. Depression of progenitor cell function by advanced glycation endproducts (AGEs): potential relevance for impaired angiogenesis in advanced age and diabetes. *Experimental Gerontology* 41: 540–548.

35. Kawamura, Y., Y. Uchijima, N. Horike, K. Tonami, K. Nishiyama, T. Amano, T. Asano, Y. Kurihara, and H. Kurihara. 2010. SIRT3 protects in vitro-fertilized mouse preimplantation embryos against oxidative stress-induced p53-mediated developmental arrest. *Journal of Clinical Investigation* 120: 2817–2828.

36. Someya, S., W. Yu, W.C. Hallows, J. Xu, J.M. Vann, C. Leeuwenburgh, M. Tanokura, J.M. Denu, and T.A. Prolla. 2010. SIRT3 mediates reduction of oxidative damage and prevention of age-related hearing loss under caloric restriction. *Cell* 143: 802–812.